



Effect of multiple coulomb scattering on the beam tests of silicon pixel detectors

Lan-Kun Li^{1,2} · Ming-Yi Dong^{2,3} · Ze Gao^{1,2} · Liang-Cheng-Long Jin^{2,4} · Shu-Jun Zhao¹

Received: 17 November 2023 / Revised: 19 January 2024 / Accepted: 23 February 2024 / Published online: 24 May 2024

© The Author(s), under exclusive licence to China Science Publishing & Media Ltd. (Science Press), Shanghai Institute of Applied Physics, the Chinese Academy of Sciences, Chinese Nuclear Society 2024

Abstract

In the research and development of new silicon pixel detectors, a collimated monoenergetic charged-particle test beam equipped with a high-resolution pixel-beam telescope is crucial for prototype verification and performance evaluation. When the beam energy is low, the effect of multiple Coulomb scattering on the measured resolution of the Device Under Test (DUT) must be considered to accurately evaluate the performance of the pixel chips and detectors. This study aimed to investigate the effect of multiple Coulomb scattering on the measured resolution, particularly at low beam energies. Simulations were conducted using Allpix² to study the effects of multiple Coulomb scattering under different beam energies, material budgets, and telescope layouts. The simulations also provided the minimum energy at which the effect of multiple Coulomb scattering could be ignored. Compared with the results of a five-layer detector system tested with an electron beam at DESY, the simulation results were consistent with the beam test results, confirming the reliability of the simulations.

Keywords Silicon Pixel Detectors · Beam Telescope · Multiple Coulomb Scattering · Spatial Resolution

1 Introduction

Vertex detectors and tracking systems play important roles in high-energy-physics experiments. Detectors with high measurement accuracy are crucial for identifying and measuring secondary particles or the decay products of short-lived particles. Silicon pixel sensors [1, 2], especially CMOS Monolithic Active Pixel Sensors (MAPS) [3], which integrate the sensor and front-end electronics readout logic on the same silicon substrate, provide high spatial resolution, high

counting rates, and good radiation hardness. Silicon pixel detectors based on MAPS have been successfully applied in vertex detectors and tracking systems, such as the vertex detector for STAR experiments at the RHIC [4] and the Inner Tracking System (ITS) Upgrade for the ALICE experiments at the LHC [5]. A MAPS-based vertex detector for the Circular Electron-Positron Collider (CEPC) has also been proposed, and significant progress has been made in the study of sensor and detector prototypes [6–9]. In addition to high-energy physics experiments, technologies related to silicon pixel detectors are widely used in other fields, such as the photon-counting pixel detector developed for the High-Energy Photon Sources (HEPS) [10–12] and digital tomography detectors used in medical applications [13].

In the R & D of new silicon pixel chips and detector prototypes, radioactive sources and cosmic rays [14–16] are widely used to verify the chip design and detector functionality. However, these laboratory tests have limitations in accurately evaluating the performance of silicon pixel chips and detectors because of the energy constraints of radioactive sources and the limited efficiency of cosmic rays. Therefore, collimated monoenergetic charged-particle test beams are commonly employed to evaluate detector performance. Test beams provide a more accurate evaluation of spatial

This work was supported by the National Natural Science Foundation of China (Nos.11875274 and U1232202).

✉ Ming-Yi Dong
dongmy@ihep.ac.cn

¹ School of Physics and Microelectronics, Zhengzhou University, Zhengzhou 450001, China

² State Key Laboratory of Particle Detection and Electronics(Institute of High Energy Physics, CAS), Beijing 100049, China

³ University of Chinese Academy of Science, Beijing 100049, China

⁴ University of South China, Hengyang 421001, China

resolution and detection efficiency and can also be used for the calibration and optimization of detector prototypes. The Beam telescope, a necessary device in the test beam, provides precise reference particle tracks for the device under test (DUT) and requires higher measurement accuracy than the DUT itself. Several beam telescopes with different test beams have been used to study new detectors. EUDET-type beam telescopes [17] consisting of six pixel detector planes equipped with MIMOSA26 chips have been replicated, such as the ACONITE telescope at CERN SPS with 120 GeV pions, the DATURA telescope at the DESY II Test Beam Facility with electrons up to 6 GeV, and the ANEMONE telescope at Bonn with 1–3 GeV electrons. ADENIUM, a demonstration of the next-generation beam telescope at DESY [18]. LYCORIS, a six-plane large-area strip-beam telescope, was installed at the DESY II Test Beam Facility and includes a 1T solenoid magnet [19]. A CMS pixel-based telescope was built at the Fermilab test-beam facility (FTBF) [20]. The construction of a beam telescope was proposed for a proton test beam of 1.6 GeV in the China Spallation Neutron Source (CSNS) [21–23].

The measurement accuracy of the detector with the test beam is strongly influenced by the beam parameters and telescope performance. In particular, when the beam energy is low and the DUT has a large material budget, it is crucial to consider the effect of multiple Coulomb scattering on the measured resolution to improve the precision of the performance evaluation of the pixel chips and detector prototypes. This study investigated the effects of multiple Coulomb scattering on the measured resolution of DUTs under different beam energies and material budgets. This will provide references for the research and testing of particle detectors and the design of beam telescopes, assisting in the selection of appropriate test beams based on the material budgets of the DUTs and minimizing the effect of multiple Coulomb scattering on the resolution. In Sect. 2, we briefly introduce the beam telescope. In Sect. 3, we study the effect of multiple Coulomb scattering using Allpix² with different beam energies, material budgets, and telescope layouts to determine the minimum energy at which the effect of multiple Coulomb scattering can be ignored. A comparison between the simulation and beam test results is presented in Sect. 4, which validates the reliability of the simulation.

2 Beam telescope

2.1 Telescope system

A beam telescope is a tracking detector system that typically comprises four or more planes with silicon pixel sensors. The pixel sensors on each plane must be thin

and highly granular. To minimize the effect of multiple Coulomb scattering, the detection area typically includes only a silicon pixel sensor and two layers of Kapton film for light shielding. A schematic of the beam telescope is shown in Fig. 1. The DUT is generally positioned at the center of the beam telescope with high-energy charged particles traversing both the telescope planes and the DUT. Generally, a mechanical structure consisting of two symmetrical telescope arms is used to support telescope planes. Both arms are adjustable along the beam direction, facilitating the easy installation of DUTs of different sizes.

In the data analysis of beam tests, detector alignment is important for calibrating the position of the DUT and each plane of the telescope by minimizing the track residuals through a large number of tracks [24]. After the alignment, the reference tracks can be reconstructed using the minimum χ^2 matrix algorithm [25]. For low-energy beams, the effect of multiple Coulomb scattering on the measured resolution cannot be ignored, particularly in the case of the non-negligible material budget of the DUT. Algorithms such as the Kalman Filter with a covariance matrix generated by multiple Coulomb scattering [26, 27] or General Broken Lines [28] can be utilized for track fitting and detector alignment to mitigate the effect of multiple Coulomb scattering. In this study, to avoid the differences caused by the algorithms, we used the same alignment algorithm as in [24] and the Kalman filter track fitting as in [26] for both the simulation and beam test data.

2.2 Measured resolution

The fitting points of the DUT can be obtained via track fitting. The measured spatial resolution of the DUT, which is the measured residual between the fitting points and the measured points, is unbiased if no DUT information is considered during track fitting. The measured resolution σ_{meas} includes contributions [29] from the intrinsic resolution of the DUT σ_{DUT} , telescope resolution σ_{tel} and the effect of multiple Coulomb scattering σ_{MS} , as described by Eq. (1):

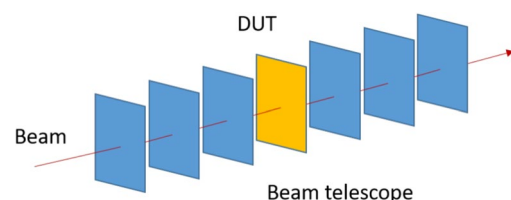


Fig. 1 (Color online) Schematic of the beam telescope with six telescope planes and the DUT

$$\sigma_{\text{meas}}^2 = \sigma_{\text{DUT}}^2 + \sigma_{\text{tel}}^2 + \sigma_{\text{MS}}^2 \tag{1}$$

Notably, the effect of multiple Coulomb scattering originates not only from the DUT but also from the telescope planes. Therefore, telescope planes are typically designed to be as thin as possible to minimize the effects of multiple Coulomb scattering.

The telescope resolution σ_{tel} can be determined if all telescope planes have the same intrinsic resolution σ_{plane} and the DUT is placed at $z = 0$, using Eq. (2) and Eq. (3):

$$\sigma_{\text{tel}}^2 = k\sigma_{\text{plane}}^2 \tag{2}$$

$$k = \frac{\sum_i^N z_i^2}{N \sum_i^N z_i^2 - (\sum_i^N z_i)^2} \tag{3}$$

where z_i and N represent the position in the beam direction and the number of telescope planes, respectively. If the telescope planes are parallel and symmetrically distributed on both sides of the DUT, then k is reduced to $1/N$.

When the beam energy is sufficiently high, the effect of multiple Coulomb scattering can be ignored, and it is assumed that the DUT and telescope planes are identical, by combining Eq.(1), Eq.(2) and Eq.(3), σ_{DUT} and σ_{tel} can be calculated from measured resolution σ_{meas} , using Eq. (4) and Eq. (5):

$$\sigma_{\text{DUT}}^2 = \frac{\sigma_{\text{meas}}^2}{1 + k} \tag{4}$$

$$\sigma_{\text{tel}}^2 = \frac{k}{1 + k} \sigma_{\text{meas}}^2 \tag{5}$$

Based on Eq. (1), the measurement result of the DUT is influenced by both the resolution of the beam telescope and the effect of multiple Coulomb scattering. However, for the silicon pixel chips of a telescope, the chip design and resolution are constrained by multiple factors and cannot be significantly improved. Therefore, evaluating and minimizing the effect of multiple Coulomb scattering is crucial for improving the measurement accuracy of DUT with beam tests.

2.3 Simulation setup

We use Allpix² [30] to simulate the test beam system and study how multiple Coulomb scattering influences the measured resolution. Allpix² is an open-source software framework written in C++, built on Geant4 and ROOT, and specifically designed for simulating silicon pixel detectors. It can easily simulate both individual detectors

and more complex systems such as test beam systems, providing detailed information such as pixel charge collection and digitized responses.

Unless otherwise stated, all simulations in this study were conducted with the following settings: the beam telescope consisted of four telescope planes, divided into two upstream and two downstream planes. The DUT was positioned at the center of the telescope. The gap between the telescope planes and the distance from the DUT to the front and rear telescope planes were set to 20 mm. The DUT and telescope planes use the same model, which consists of a MIMOSA28 chip [31] thinned to 50 μm and two layers of 50 μm Kapton film, resulting in a total material budget of 0.088% X_0 per plane. The MIMOSA28 chip contains 928 (row) × 960 (column) pixels with a pitch of 20.7 μm. It has a 15 μm-thick high-resistivity epitaxial layer as a sensitive layer that is not fully depleted, thus allowing charge collection through thermal diffusion. MIMOSA28 chips are also being considered for use in the upcoming proton beam telescopes on CSNS. In this simulation, the electronic noise of the chip was set to 30 e^- based on the threshold scan results, and the threshold was set to 5 σ to mitigate the influence of the electronic noise and achieve optimal resolution.

3 Multiple Coulomb scattering

When charged particles pass through materials, they suffer many small-angle deflections, known as multiple Coulomb scattering. The Highland formula [32] can be used to calculate the distribution of the multiple Coulomb scattering angles θ_0 , as Eq.(6)

$$\theta_0 = \frac{13.6 \text{ MeV}}{\beta c p} Z \sqrt{\frac{x}{X_0}} \left(1 + 0.038 \ln \left(\frac{x}{X_0} \right) \right), \tag{6}$$

where p is the momentum of the incident particles, βc is the velocity, and Z is the number of charged particles. x/X_0 indicates the material budget, where x and X_0 represent the track length of the particles passing through the material and the radiation length of the material, respectively. Multiple Coulomb scattering originating from both the beam telescope planes and the DUT degrade the measured resolution of the DUT.

As Eq. (6), the beam energy and the material budget can both influence multiple Coulomb scattering angles θ_0 . In addition, for the same θ_0 , the effect of multiple Coulomb scattering is influenced by the distance between the two measurement points. Therefore, three factors can influence the effect of multiple Coulomb scattering: the beam energy, material budget, and telescope layout.

3.1 Beam energy

To study the impact of the beam energy on the multiple Coulomb scattering angle and, consequently, the simulation result of the resolution (σ_{meas}), represented as the simulated resolution in the following, we simulated different electron beam energies from 0.5 GeV to 30 GeV, and the DUT was the same as the plane model of the telescope with a material budget of $0.088\% X_0$. Based on Eq. (6), with this system setting, when the beam energy is high enough, for example, 120 GeV, the effect of multiple Coulomb scattering can be ignored. Therefore, a beam energy of 120 GeV can be used as the reference without the effect of multiple Coulomb scattering. Figure 2 shows the simulated resolution as a function of beam energy. Increasing the beam energy can significantly improve resolution in the low-energy range. When the beam energy is sufficiently large, the simulated resolution no longer improves and approaches the value of 120 GeV electrons. Therefore, the effect of multiple Coulomb scattering at different energies can be calculated using Eq. (1). When the beam energy was greater than 12 GeV, σ_{MS} was less than $0.5 \mu\text{m}$. Compared with the value achieved with 120 GeV electrons, the simulated resolution with 12 GeV experiences a degradation of less than 1%.

3.2 Material budget

Beam telescopes are typically designed to minimize the material budget, making the material budget of the DUT the primary factor influencing the effects of multiple Coulomb scattering. Thus, to study the impact of the material budget on the simulated resolution of the DUT, the material budget of the DUT is changed from $0.106\% X_0$ to $0.53\% X_0$ by increasing the equivalent thickness of silicon from $100 \mu\text{m}$ to $500 \mu\text{m}$ without Kapton films, while the material budget of each telescope plane remains $0.088\% X_0$ unchanged. Figure 3 shows the simulated resolution as a function of the

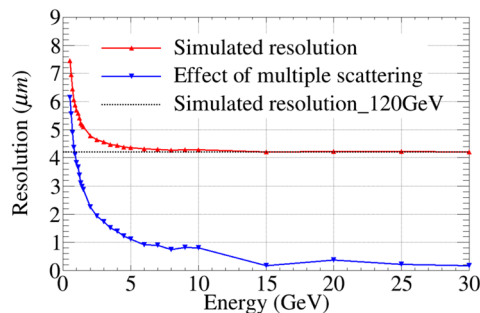


Fig. 2 Simulated resolution of the DUT as a function of the beam energy from 0.5 to 30 GeV. The dotted line shows the simulated resolution with 120 GeV electrons. The effect of multiple Coulomb scattering with different energies is calculated and shown as the blue line

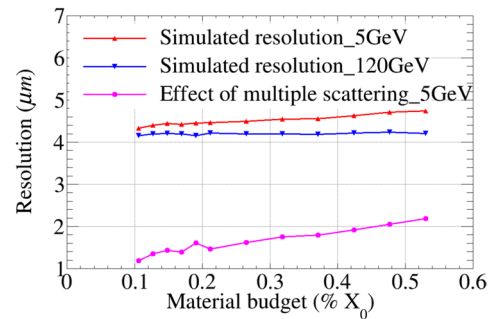


Fig. 3 Simulated resolution of the DUT as a function of the material budget with 5 GeV and 120 GeV electrons. The material budgets of the DUT models change from $0.106\% X_0$ to $0.53\% X_0$. The effect of multiple Coulomb scattering with 5 GeV electrons is calculated and represented as the purple line

material budget with 5 and 120 GeV electrons. With 120 GeV electrons, as the material budget increased, the simulated resolution remained nearly constant because the effect of multiple Coulomb scattering was sufficiently small to be ignored. However, when using 5 GeV electrons, doubling the material budget results in an increase of approximately 25% in the effect of multiple Coulomb scattering and degradation of the simulated resolution by approximately 5%.

Based on the above conclusions, the simulated resolution with 120 GeV electrons (approximately $4.18 \mu\text{m}$) can be used as a reference for studying the effects of multiple Coulomb scattering with different material budgets and beam energies. This allows the estimation of the minimum energy at which the effect of multiple Coulomb scattering can be ignored for different material budgets of the DUT. We changed the material budget of the DUT from $0.106\% X_0$ to $1.06\% X_0$ at energies ranging from 5 to 50 GeV. Figure 4 shows the effect of multiple Coulomb scattering as a function of beam energy for different DUT models. Increasing the beam energy significantly reduced the effect of multiple

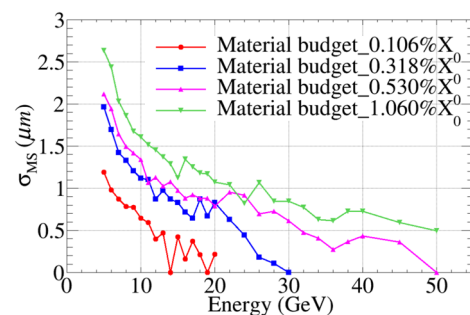


Fig. 4 Effect of multiple Coulomb scattering as a function of the beam energy from 5 to 50 GeV. The models of the DUT have different material budgets from $0.106\% X_0$ to $1.06\% X_0$, while the material budget of telescope planes remains $0.088\% X_0$ unchanged

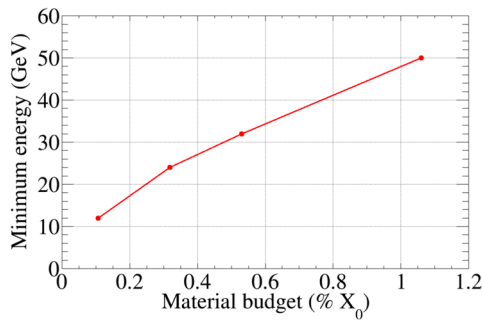


Fig. 5 Minimum energy as a function of the material budget of the DUT. When the beam energy is larger than the minimum energy, the contribution of the effect of multiple Coulomb scattering is less than $0.5 \mu\text{m}$, causing a decrease of less than 1% in σ_{meas} , which can be ignored

Coulomb scattering. When σ_{MS} was less than $0.5 \mu\text{m}$, the resolution of the DUT decreased by less than 1%. Therefore, the simulated resolution of the DUT is influenced more by the randomness of the simulation and statistical errors, resulting in fluctuations in the curves of σ_{MS} at high beam energies, as shown in Figs. 2 and 4. Figure 5 shows the minimum energy at which the effect of multiple Coulomb scattering can be ignored as a function of the various DUT material budgets. The minimum energy increases as the material budget of the DUT increases.

3.3 Telescope layout

The telescope arms can be adjusted in the beam direction to modify the distance between the DUT and telescope planes, allowing the testing of various device sizes. Modifying the layout influences the effect of multiple Coulomb scattering even if the multiple Coulomb scattering angle θ_0 remains constant. Furthermore, altering the number of beam telescope planes affects the factor k in Eq.(2) and the effect of multiple Coulomb scattering. To study these impacts, we conducted simulations with a 4-layer, 5-layer, and 6-layer telescope with different layouts. For the 5-layer beam telescope, there were three planes before and two layers after the DUT. In the simulation, the DUT was set the same as that in the telescope plane.

The resolution of the DUT is strongly influenced by the distance between the DUT and the nearest telescope planes. As shown in Fig. 6(a), the simulation results indicate that reducing the gap between the DUT and telescope planes within the range of 10–100 mm can improve the simulated resolution. Increasing the track length resulted in a larger measured residual between the fitting and measured points, thereby degrading

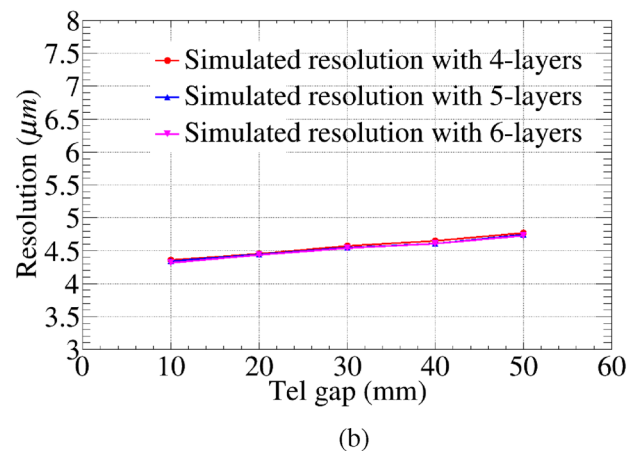
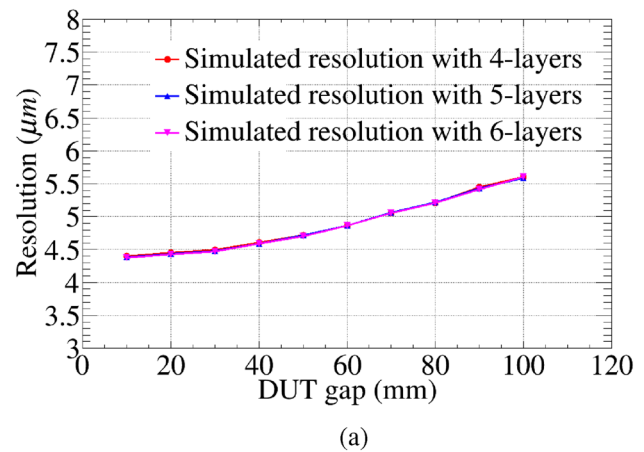


Fig. 6 (a) Simulated resolution of the DUT as a function of the distance from the DUT to both the front and rear telescope planes, simulated with 5 GeV electrons. The gap between telescope planes is kept 20 mm. (b) Simulated resolution of the DUT as a function of the distance between telescope planes simulated with 5 GeV electrons. The distance from the DUT to both the front and rear telescope planes is kept 20 mm

the simulated resolution. However, the distance between the DUT and the telescope is limited by the size of the DUT. For DUTs of varying sizes, minimizing the gap between the DUT and nearest telescope planes is crucial for achieving a better resolution. Figure 6(b) shows the simulated resolution as a function of the distance between the telescope planes. Minimizing the distance between the telescope planes can reduce the effect of multiple Coulomb scattering. Theoretically, increasing the number of telescope planes can improve telescope resolution, as shown in Eq. (5). However, this increases the total material budget of the beam telescope. With 5 GeV electrons, the simulated resolution with a 4-layer telescope is essentially the same as the resolution with a 6-layer telescope.

4 Comparison between simulation and test results

To validate the accuracy of the simulation, we compared the simulation results with the beam test results of a detector system comprising five ladders [33, 34], as shown in Fig. 7. In the beam test system, each ladder consists of MIMOSA28 chips thinned to $50\ \mu\text{m}$, a flex cable, and a 1.8 mm thick carbon fiber and foam composite support, resulting in a material budget of approximately $0.35\% X_0$. In this test system, the first and last two layers can be used as a telescope, and the ladder in the middle can be used as a DUT, which has been tested at the T24 beamline at DESY, with beam energies ranging from 1 to 6 GeV. In the

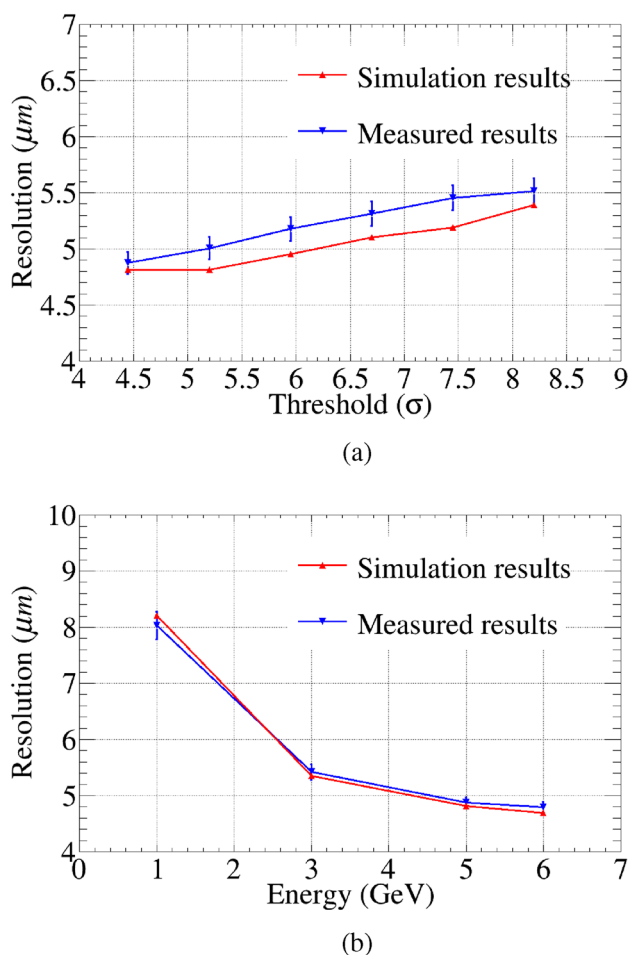


Fig. 7 Comparison between the resolutions of test results and simulation results. (a) Resolutions of test and simulation results as a function of the threshold from $4.45\ \sigma$ to $8.2\ \sigma$. (b) Resolution of test results and simulation results as a function of the beam energy from 1 to 6 GeV. The threshold of the DUT is $4.45\ \sigma$. The error bar represents the systematic uncertainty, including the beam energy dispersion 5% and the prediction accuracy of the multiple Coulomb scattering angle θ_0

simulation, the method mentioned in the previous sections was adopted, and the model was identical to the real ladder. The same algorithms used in the simulation were used for the test data analysis.

Figure 7(a) shows the measured resolution as a function of the threshold from $4.45\ \sigma$ to $8.2\ \sigma$. The threshold range is determined using threshold scans. If the threshold is too low, fake hits caused by electronic noise will impact track fitting and reconstruction, and spatial resolution. The simulation results were slightly smaller than the measured resolution from the beam test, primarily because some factors, such as beam energy dispersion and slightly different noises of different chips, were not considered in the simulation. Figure 7(b) shows the measured resolution as a function of beam energy, ranging from 1 to 6 GeV. Based on the test results, the contribution of the multiple Coulomb scattering effect at 5 GeV was approximately $2.7\ \mu\text{m}$ because of the relatively large material budget of the ladders. The simulation and actual beam test results exhibited consistency across different thresholds and beam energies.

5 Conclusion

The effect of multiple Coulomb scattering on the measured resolution of the DUT under different beam energies, material budgets, and telescope layouts was studied through simulations using Allpix². The simulation results are consistent with the beam test results, thereby confirming the reliability of the simulations. The effect of multiple Coulomb scattering depends on three main factors: the beam energy, material budget, and telescope layout. Increasing the beam energy or reducing the material budget can effectively mitigate the effects of multiple Coulomb scattering. For beam energy of 5 GeV and material budget of the DUT ranging from $0.1\% X_0$ to $0.5\% X_0$, the effect of multiple Coulomb scattering is approximately $1\text{--}2\ \mu\text{m}$. When the beam energy is sufficiently high, the resolution of DUT remains unchanged as the energy increases because the effect of multiple Coulomb scattering can be ignored. When the material budget of the DUT is less than $0.2\% X_0$, the minimum energy at which the effect of multiple Coulomb scattering could be ignored is approximately 20 GeV, which increases as the material budget of the DUT increases. Additionally, the resolution of the DUT is significantly influenced by the distance between the DUT and the nearest telescope planes. Reducing the gap between the DUT and telescope planes to within the range of 10–100 mm can improve the measured resolution. To accurately evaluate the performance of DUTs with different sizes, it is essential to minimize the gap between the DUT and the nearest telescope planes. The results can provide a reference for the selection

of an appropriate test beam energy for DUTs with different material budgets and for the design of a test beam telescope.

Acknowledgements The measurements leading to these results have been performed at the Test Beam Facility at DESY Hamburg (Germany), a member of the Helmholtz Association (HGF).

Author Contributions All authors contributed to the study conception and design. Material preparation, data collection and analysis were performed by Lan-Kun Li, Ming-Yi Dong and Ze Gao. The first draft of the manuscript was written by Lan-Kun Li and all authors commented on previous versions of the manuscript. All authors read and approved the final manuscript.

Data Availability Statement The data that support the findings of this study are openly available in Science Data Bank at <https://cstr.cn/31253.11.sciencedb.j00186.00476> and <https://doi.org/10.57760/sciencedb.j00186.00476>.

Declaration

Conflict of interest The authors declare that they have no Conflict of interest.

References

1. R. He, X.Y. Niu, Y. Wang et al., Advances in nuclear detection and readout techniques. *Nucl. Sci. Tech.* **34**, 205 (2023). <https://doi.org/10.1007/s41365-023-01359-0>
2. S. Seidel, Silicon strip and pixel detectors for particle physics experiments. *Phys. Rep.* **828**, 1–34 (2019). <https://doi.org/10.1016/j.physrep.2019.09.003>
3. G. Deptuch, J.D. Berst, G. Claus et al., Design and testing of monolithic active pixel sensors for charged particle tracking. *IEEE Trans. Nucl. Sci.* **49**, 601–610 (2002). <https://doi.org/10.1109/TNS.2002.1003683>
4. L. Greiner, E. Anderssen, H.S. Matis et al., A MAPS based vertex detector for the STAR experiment at RHIC. *Nucl. Instrum. Meth. A* **650**, 68–72 (2011). <https://doi.org/10.1016/j.nima.2010.12.006>
5. P. Yang, G. Aglieri, C. Cavicchioli et al., MAPS development for the ALICE ITS upgrade. *J. Instrum.* **10**, C03030 (2015). <https://doi.org/10.1088/1748-0221/10/03/C03030>
6. L.J. Chen, H.B. Zhu, X.C. Ai et al., Characterization of the first prototype CMOS pixel sensor developed for the CEPC vertex detector. *Radiat. Detect. Technol. Methods.* **3**, 45 (2019). <https://doi.org/10.1007/s41605-019-0124-0>
7. S. Dong, P. Yang, Y. Zhang et al., Design and characterisation of the JadePix-3 CMOS pixel sensor. *Nucl. Instrum. Meth. A* **1048**, 167967 (2023). <https://doi.org/10.1016/j.nima.2022.167967>
8. W. Wei, T.Y. Wu, Z.J. Liang et al., Characterization of a CMOS Pixel Sensor prototype for the CEPC vertex detector. *Nucl. Instrum. Meth. A* **1056**, 168601 (2023). <https://doi.org/10.1016/j.nima.2023.168601>
9. T.Y. Wu, S.Q. Li, W. Wei et al., Beam test of a 180 nm CMOS Pixel Sensor for the CEPC vertex detector. *Nucl. Instrum. Meth. A* **1059**, 168945 (2024). <https://doi.org/10.1016/j.nima.2023.168945>
10. Z. j. Li, Y.C. Jia, L. F. Hu et al., Study of silicon pixel sensor for synchrotron radiation detection. *Chinese Phys. C* **40**, 036001 (2016). <https://doi.org/10.1088/1674-1137/40/3/036001>
11. Y. Ding, J. Zhang, W. Wei et al., The development and application of the test system for the silicon pixel modules in HEPS-BPIX. *Radiat. Detect. Technol. Methods.* **5**, 53–60 (2021). <https://doi.org/10.1007/s41605-020-00217-6>
12. J. Zhang, H.X. Li, W. Wei et al., HEPS-BPIX2: The hybrid pixel detector upgrade for high energy photon source in China. *Nucl. Instrum. Meth. A* **958**, 162488 (2020). <https://doi.org/10.1016/j.nima.2019.162488>
13. Y.L. Chen, H.K. Wang, S.Y. Zhang et al., Hi'CT: a pixel sensor-based device for ion tomography. *Nucl. Sci. Tech.* **34**, 111 (2023). <https://doi.org/10.1007/s41365-023-01251-x>
14. L. Ma, X. Dong, H. Qiu et al., Alignment calibration and performance study of the STAR PXL detector. *Nucl. Sci. Tech.* **28**, 25 (2017). <https://doi.org/10.1007/s41365-016-0177-4>
15. R. Nouicer, Y. Akiba, R. Bennett et al., Status and performance of new silicon stripixel detector for the PHENIX experiment at RHIC: Beta source, cosmic-rays and proton beam at 120 GeV. *J. Instrum.* **4**, P04011 (2009). <https://doi.org/10.1088/1748-0221/4/04/P04011>
16. C.H. Chen, Z.K. Li, X.H. Wang et al., Development of high performance PIN-silicon detector and its application in radioactive beam physical experiment. *Acta Phys. Sin.* **72**, 122902 (2023). <https://doi.org/10.7498/aps.72.20230213>
17. C. Hu-Guo, J. Baudot, G. Bertolone et al., First reticule size MAPS with digital output and integrated zero suppression for the EUDET-JRA1 beam telescope. *Nucl. Instrum. Meth. A* **623**, 480–482 (2010). <https://doi.org/10.1016/j.nima.2010.03.043>
18. Y. Liu, C.Q. Feng, I.M. Gregor et al., ADENIUM-A demonstrator for a next-generation beam telescope at DESY. *J. Instrum.* **18**, P06025 (2023). <https://doi.org/10.1088/1748-0221/18/06/P06025>
19. J. Brau, M. Breidenbach, D.R. Freytag et al., Lycoris-A large-area, high resolution beam telescope. *J. Instrum.* **16**, P10023 (2021). <https://doi.org/10.1088/1748-0221/16/10/P10023>
20. S. Kwan, C.M. Lei, D. Menasce et al., The pixel tracking telescope at the Fermilab Test Beam Facility. *Nucl. Instrum. Meth. A* **811**, 162–169 (2016). <https://doi.org/10.1016/j.nima.2015.12.003>
21. S. Wang, S.X. Fang, S.N. Fu et al., Introduction to the overall physics design of CSNS accelerators. *Chinese Phys. C* **33**, 1 (2009). <https://doi.org/10.1088/1674-1137/33/S2/001>
22. J. Wei, H.S. Chen, Y.W. Chen et al., China spallation neutron source: design, R & D, and outlook. *Nucl. Instrum. Meth. A* **600**, 10–13 (2009). <https://doi.org/10.1016/j.nima.2008.11.017>
23. S.N. Fu, H.S. Chen, Y.B. Chen et al., CSNS project construction. *J. Phys. Conf. Ser.* **1021**, 012002 (2018). <https://doi.org/10.1088/1742-6596/1021/1/012002/meta>
24. V. Karimaki, A. Heikkinen, T. Lampen et al., Sensor alignment by tracks. In: Paper presented at the 2003 Conference for Computing in High-Energy and Nuclear Physics, CA, USA, 24–28 Mar 2003. <https://doi.org/10.48550/arXiv.physics/0306034>
25. G. Lutz, Optimum track fitting in the presence of multiple scattering. *Nucl. Instrum. Meth. A* **273**, 349–361 (1988). [https://doi.org/10.1016/0168-9002\(88\)90836-4](https://doi.org/10.1016/0168-9002(88)90836-4)
26. E.J. Wolin, L.L. Ho, Covariance matrices for track fitting with the Kalman filter. *Nucl. Instrum. Meth. A* **329**, 493–500 (1993). [https://doi.org/10.1016/0168-9002\(93\)91285-U](https://doi.org/10.1016/0168-9002(93)91285-U)
27. R. Frühwirth, T. Todorov, M. Winkler, Estimation of detector alignment parameters using the Kalman filter with annealing. *J. Instrum.* **29**, 561 (2003). <https://doi.org/10.1088/0954-3899/29/3/309>
28. C. Kleinwort, General Broken Lines as advanced track fitting method. *Nucl. Instrum. Meth. A* **673**, 107–110 (2012). <https://doi.org/10.1016/j.nima.2012.01.024>
29. A. Bulgheroni, EUDET-JRA1 Consortium, Results from the EUDET telescope with high resolution planes. *Nucl. Instrum. Meth. A* **623**, 399–401 (2010). <https://doi.org/10.1016/j.nima.2010.03.015>
30. S. Spannagel, K. Wolters, D. Hynds et al., Allpix2: A modular simulation framework for silicon detectors. *Nucl. Instrum. Meth. A* **901**, 164–172 (2018). <https://doi.org/10.1016/j.nima.2018.06.020>

31. I. Valin, C. Hu-Guo, J. Baudot et al., A reticle size CMOS pixel sensor dedicated to the STAR HFT. *J. Instrum.* **7**, C01102 (2012). <https://doi.org/10.1088/1748-0221/7/01/C01102>
32. V.L. Highland, Some practical remarks on multiple scattering. *Nucl. Instrum. Methods* **129**, 497–499 (1975). [https://doi.org/10.1016/0029-554X\(75\)90743-0](https://doi.org/10.1016/0029-554X(75)90743-0)
33. M.Y. Dong, X.D. Ju, X.C. Tian et al., Development of MAPS-based detector ladders for the BESIII inner tracker upgrade. *Nucl. Instrum. Meth. A* **924**, 287–292 (2019). <https://doi.org/10.1016/j.nima.2018.06.032>
34. C.Y. Qu, M.Y. Dong, J. Baudot et al., Performance study of a MAPS detector prototype based on test beam. *Nucl. Instrum. Meth. A* **986**, 164810 (2021). <https://doi.org/10.1016/j.nima.2020.164810>

Springer Nature or its licensor (e.g. a society or other partner) holds exclusive rights to this article under a publishing agreement with the author(s) or other rightsholder(s); author self-archiving of the accepted manuscript version of this article is solely governed by the terms of such publishing agreement and applicable law.